PERGAMON

Journal of Structural Geology 25 (2003) 1883–1892

JOURNAL OF STRUCTURAL GEOLOGY

www.elsevier.com/locate/jsg

General shear deformation in the Pinaleño Mountains metamorphic core complex, Arizona

Christopher M. Bailey*, Eleanor L. Eyster

Department of Geology, College of William & Mary, Box 8795, Williamsburg, VA 23187, USA

Received 31 October 2001

Abstract

Granitic mylonites from the Pinaleño Mountains metamorphic core complex in southeastern Arizona record general shear deformation. The mean kinematic vorticity number (W_m) was estimated using (1) the strain ratio (R_s) and the angle (Θ) between the long axis of the strain ellipsoid with respect to the high-strain zone boundary and (2) the porphyroclast hyperbolic distribution method. W_m for protomylonites and mylonites ranged from 0.6 to 0.9. Ultramylonites record lower W_m values (0.1–0.3) suggesting that the incremental vorticity changed during deformation. Three-dimensional strain analysis indicates that deformation in protomylonites and mylonites approximates plane strain and has a monoclinic symmetry. The vorticity path followed by rocks tectonically exhumed in the footwall of major extensional fault systems may evolve from a significant pure shear component early in the deformation towards simple shear as overburden load decreases during uplift.

Keywords: Mylonites; Vorticity; Shear zone; Metamorphic core complex

1. Introduction

Structural geologists have traditionally been concerned with trying to understand the kinematics, deformation conditions, and tectonic significance of high-strain zones. Over the past 15 years a number of techniques have been developed to quantitatively evaluate both strain and vorticity in deformed rocks (Passchier, 1987; Passchier and Urai, 1988; Simpson and De Paor, 1993; Tikoff and Teyssier, 1994). However, relatively few studies have quantified the strain and vorticity path in naturally deformed rocks (see, however, Wallis, 1992; Simpson and De Paor, 1997; Beam and Fisher, 1999).

Homogeneous plane strain deformation has traditionally been described by the distinct end-member flow patterns: pure shear and simple shear, with the general shear condition representing intermediate states between pure and simple shear deformation. A measure of the non-coaxiality of deformation is given by the kinematic vorticity number (W_n), which records the amount of rotation relative to the amount of stretching (Passchier, 1988a). For pure shear flow $W_n = 0$ and for simple shear flow $W_n = 1$. W_n is a measure of the instantaneous vorticity of flow, while the related quantity W_m is a measure of the mean vorticity of deformation (Passchier, 1988a,b). For steady-state progressive deformation $W_n = W_m$. In naturally deformed rocks geologists encounter the final products of deformation and commonly can only estimate finite quantities (i.e. W_m not W_n) rather than uniquely characterizing the progressive history of deformation.

In a three-dimensional deformation the kinematic vorticity number does not uniquely describe the flow conditions (Tikoff and Fossen, 1995). However, W_n can be meaningful if used in conjugation with an understanding of the boundary conditions and the three-dimensional strain geometry (constriction, plane strain, or flattening) (Tikoff and Fossen, 1995). In an attempt to categorize all possible combinations of three-dimensional strain with a component of orthogonal simple shear, Tikoff and Fossen (1999) recognized 12 end-member reference deformations. Traditionally, flow in high-strain zones has been considered to have a monoclinic symmetry; however, Lin et al. (1998) and Jiang and Williams (1998) demonstrated that triclinic deformation symmetries are common and suggest that

* Corresponding author. Tel.: +1-757-221-2440; fax: +1-757-221-2093. *E-mail address:* cmbail@wm.edu (C.M. Bailey).

0191-8141/03/$ - see front matter © 2003 Elsevier Ltd. All rights reserved.
doi:10.1016/S0191-8141(03)00044-0

simple monoclinic symmetries are the exception rather than the rule.

Cordilleran metamorphic core complexes in the southwestern United States are characterized by curvi-planar zones of mylonitic rocks that separate mid-crustal igneous and metamorphic rocks of the lower plate from supracrustal materials in the upper plate. The style of deformation in the ductily deformed rocks of the lower plate is controversial. Many workers consider deformation to have approximated simple shear in these extensional high-strain zones (Davis, 1983; Reynolds, 1985; Davis et al., 1986; Naruk, 1986, 1987). However, coaxial (low W_m) fabrics have also been reported in a number of metamorphic core complexes (Compton, 1980; Miller et al., 1983; Lee et al., 1987; Wells and Allmendinger, 1990; Bestmann et al., 2000). In the Pinaleño Mountains metamorphic core complex of southeastern Arizona, Naruk (1986, 1987) used the angular discordance between planar fabrics and the deflection of geologic contacts as evidence for a bulk simple shear, plane strain deformation path. In this study we combine recent advances with traditional strain analysis methods to quantitatively understand the kinematics in the Pinaleño Mountains high-strain zone. Our work indicates that mylonitic rocks from the Pinaleño Mountains high-strain zone record a bulk plane strain deformation that developed under general shear conditions characterized by a monoclinic symmetry.

2. Geologic setting

The Pinaleño Mountains are a northwest-trending range in southeastern Arizona near the edge of the Basin and Range province (Fig. 1). The range is underlain primarily by Proterozoic (1.7–1.1 Ga) metamorphic rocks and middle Cenozoic plutons (Thorman, 1982; Davis et al., 1988; Long et al., 1995). A zone of mylonitic rocks flanks the northeastern side of the Pinaleño Mountains and separates the metamorphic and igneous complex from late Cenozoic sediments of the Gila Valley (Naruk, 1986). Mylonitic rocks, derived from granitic and gneissic rocks in the core of the range, strike NW–SE, dip gently to the NE, and form a high-strain zone at least 0.5–1 km thick. Kinematic indicators record top-to-the-northeast movement associated with Basin and Range extension and core complex development (Naruk, 1986, 1987). Naruk (1987) estimated a minimum displacement of 3–7 km across the Pinaleño Mountains high-strain zone by integrating shear strain assuming simple shear deformation. $^{40}Ar/^{39}Ar$ cooling ages for Pinaleño Mountains mylonites range from 19 to 29 Ma (Long et al., 1995). Seismic data from the Gila Valley, to the northeast of the Pinaleño Mountains, indicate that mylonitic rocks extend from the surface into the mid-crust (Kruger and Johnson, 1994).

We estimated strain and vorticity for a segment of the Pinaleño Mountains high-strain zone where granite and granodiorite (White Streaks pluton of Naruk (1983)) are transformed into protomylonite, mylonite, and narrow (< 10 cm) localized zones ultramylonite. The lower boundary of the high-strain zone is a 10–20-m-thick transitional zone between mylonitic rocks and unfoliated massive granitic rocks (Fig. 2). This boundary is approximately planar over kilometer-scale domains, strikes ~300° and dips 35 ± 3° NE (Fig. 1) (Naruk, 1986). Mylonitic (s-surfaces) foliation in the high-strain zone strikes 285–330° and dips 20–35° NE. Shear bands (*C*-surfaces) are developed in some of the mylonitic rocks and dip 5–15° more steeply than the foliation. A penetrative elongation lineation plunges 12–33° to the NE. The upper boundary of the high-strain zone is not exposed as mylonitic rocks are unconformably overlain by Neogene alluvial sediments (Fig. 1). The mylonitic foliation is cross-cut by discrete, planar normal faults related to Basin and Range extension (Naruk, 1986).

3. Strain and vorticity estimates

Granitic rocks beneath the lower high-strain zone boundary are massive and composed of plagioclase, quartz, K-feldspar, biotite, and minor hornblende with accessory epidote, sphene, and muscovite. Quartz forms irregular-shaped blebs with patchy undulose extinction and aspect ratios of up to 2:1 (Fig. 3A). Although many individual quartz grains are inequant, collectively these grains do not define a grain shape preferred orientation (GSPO). In the high-strain zone, quartz has been transformed into lenses and ribbons with aspect ratios of 2:1 to > 20:1 (Figs. 3B and C and 4). Quartz grains are commonly polycrystalline aggregates. Individual grains within polycrystalline lenses and ribbons are 150–400 μm in diameter, have irregular grain boundaries, define a moderate GSPO, and display a crystallographic preferred orientation. Quartz microstructures are indicative of dynamic recrystallization by both subgrain rotation and grain boundary migration (Regimes II and III of Hirth and Tullis (1992)). Feldspars display a range of microstructures including deformation twins, flame perthite, patchy undulose extinction, and asymmetric myrmekite. In some samples original igneous feldspars are mantled by fine-grained (< 50 μm) aggregates indicative of minor dynamic recrystallization by subgrain rotation (Tullis and Yund, 1985). Crystal-plastic feldspar microstructures are commonly cut by intra- and inter-granular fractures. Ultramylonites are characterized by a fine-grained matrix of quartz, biotite, and muscovite with 10–20%-rounded porphyroclasts of plagioclase and K-feldspar (Fig. 3D). Quartz and feldspar microstructures are consistent with peak deformation conditions in the upper greenschist facies (~450 °C) (Tullis, 1983; Tullis and Yund, 1987; Simpson and Wintsch, 1989).

Strain was estimated from quartz grain shapes using the R_f/ϕ_f method with a hyperbolic stereonet (De Paor, 1988)

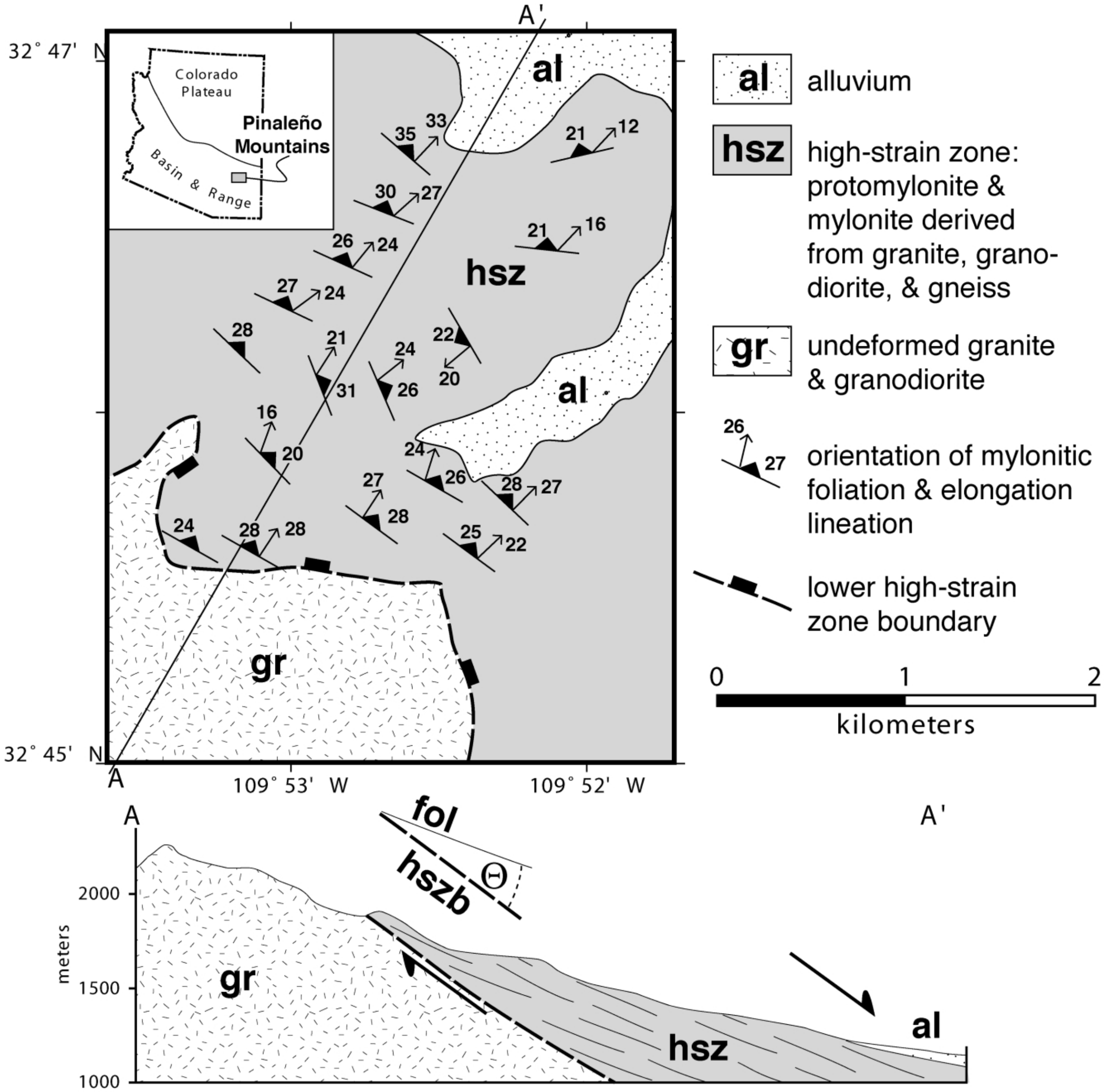

Fig. 1. Geologic map and cross-section of the Ash Creek and White Streaks Canyon area, Pinaleño Mountains, Arizona. The angle between the high-strain zone boundary (hszb) and foliation (fol) is Θ.

(Fig. 4, Table 1). Although quartz grains have internally recrystallized during deformation their margins are distinct and clearly defined by other phases (Fig. 3B and C). Quartz has been used as a strain marker in a number of greenschist facies high-strain zones (Mawer, 1983; O'Hara, 1990; Bailey et al., 1994; Fletcher and Bartley, 1994). Bailey et al. (1994) demonstrated that quartz grain shapes record strain ratios similar to fractured and boudinaged feldspar grains from the same samples. At low and medium metamorphic grades, granitic mylonites are composed of three mechanically different phases: feldspar, quartz, and mica. In most situations feldspar is the strongest phase and mica the weakest; thus strain estimates based on quartz grain shapes may be suitable for approximating whole rock strain at the scale of a thin section or hand sample. Our strain estimates (Table 1) from quartz grain shapes are comparable with the strains estimated from deflected planar markers in the Pinaleño Mountains high-strain zone by Naruk (1986). Strain estimates based on grain shapes cannot resolve strain due to grain boundary sliding (Wenk and Pannetier, 1990), thus at high strains in mica-rich mylonites our strain estimates may be low. However, in low- to moderate-strain protomylonites and mylonites the framework feldspars are still in contact with one another and grain boundary sliding should be minimal.

Below the high-strain zone boundary, quartz grain shapes

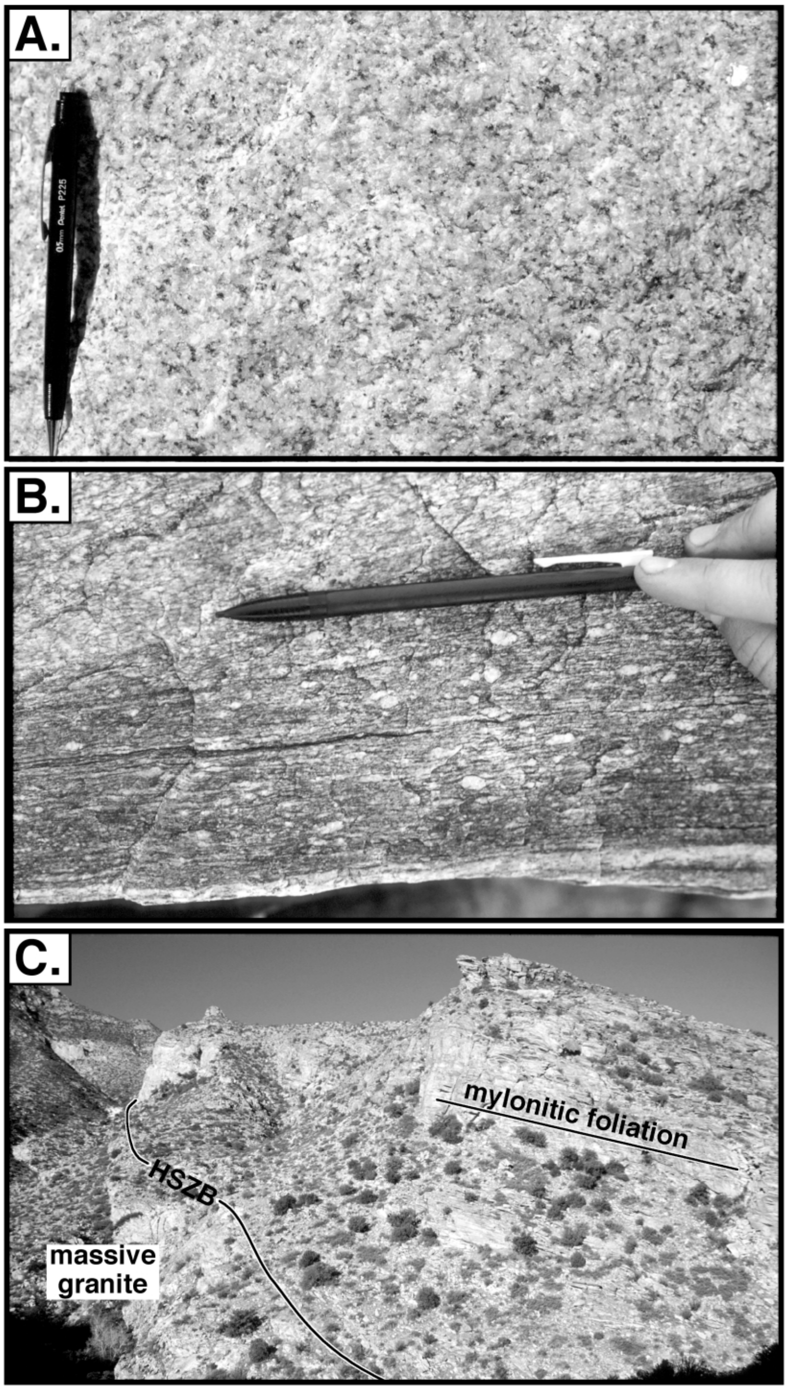

Fig. 2. (A) Undeformed White Streaks granodiorite approximately 50 m below the lower high-strain zone boundary. (B) Porphyroclastic mylonite derived from White Streaks granodiorite. (C) View to west-northwest of the lower high-strain zone boundary (HSZB) separating undeformed White Streaks granodiorite (left) from mylonitic rock in the high-strain zone (right). Mylonitic foliation dips less steeply than the high-strain zone boundary.

from three samples yield sectional strain ratios of ~ 1.1 with no systematic orientation of the long axis. In protomylonites and mylonites, sections were measured parallel to lineation and normal to foliation as well as normal to both foliation and lineation. In each section, 16–60 quartz grains were measured. The long axis of the sectional strain ellipse is always within 5° of the macroscopic fabric element suggesting that the macroscopic foliation (*S*-surfaces) defines a principal plane of the finite strain ellipsoid (Fig. 4). Strain ratios in *XZ* sections ranged from two to eight (Table 1). Three-dimensional strains generally plot near the line of plane strain on a Flinn diagram (Fig. 5). Pegmatitic veins generally showed no evidence for either contraction or extension in planes normal to the elongation lineation, consistent with a bulk plane strain deformation. Naruk (1986) reports geochemical evidence from the granitic

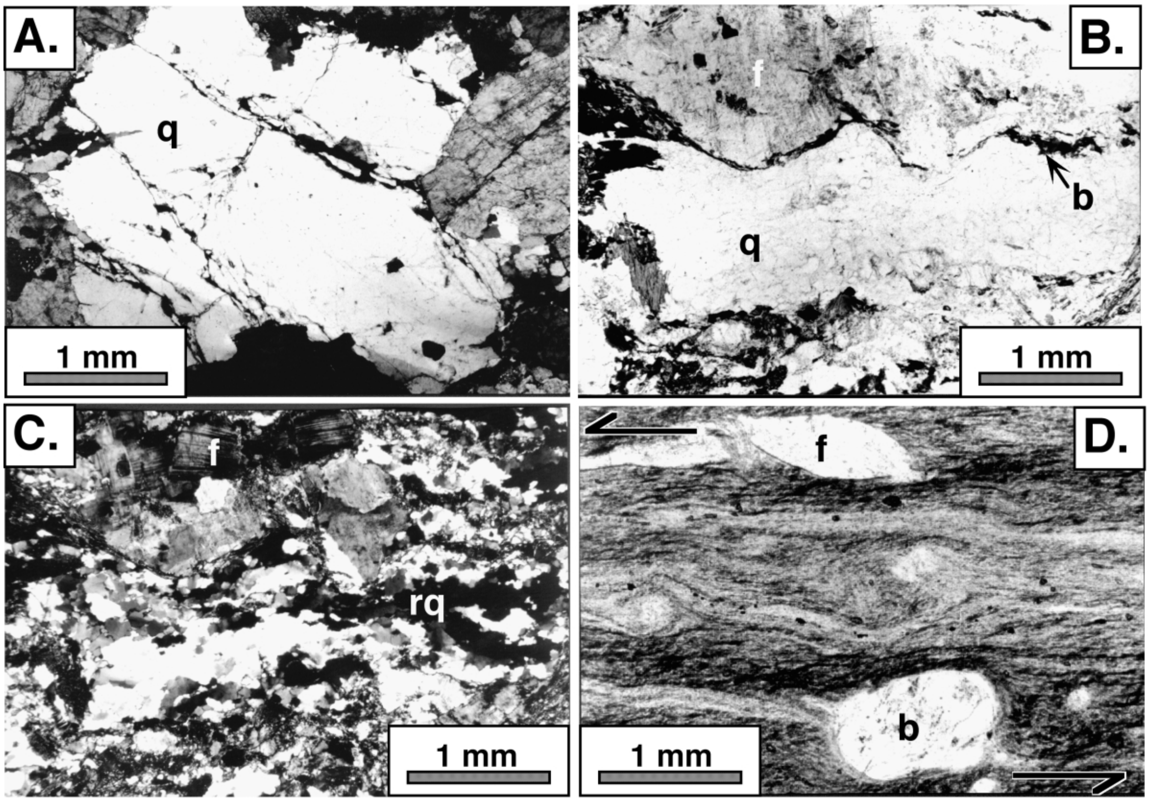

Fig. 3. Photomicrographs of (A) irregular quartz (q) lens in macroscopically undeformed granite below the lower high-strain zone boundary (XPL). (B) Elongate quartz (q) lens with an aspect ratio of ~5:1 in granitic mylonite (PPL). Edge of the quartz lens defined by biotite (b) and feldspar (f). (C) Same quartz lens as (B) (XPL). Quartz lens is composed of an aggregate of dynamically recrystallized grains (rq). (D) Forward (f) and backward (b) rotated feldspar porphyroclasts in ultramylonite (PPL). Top-to-the-left sense of shear.

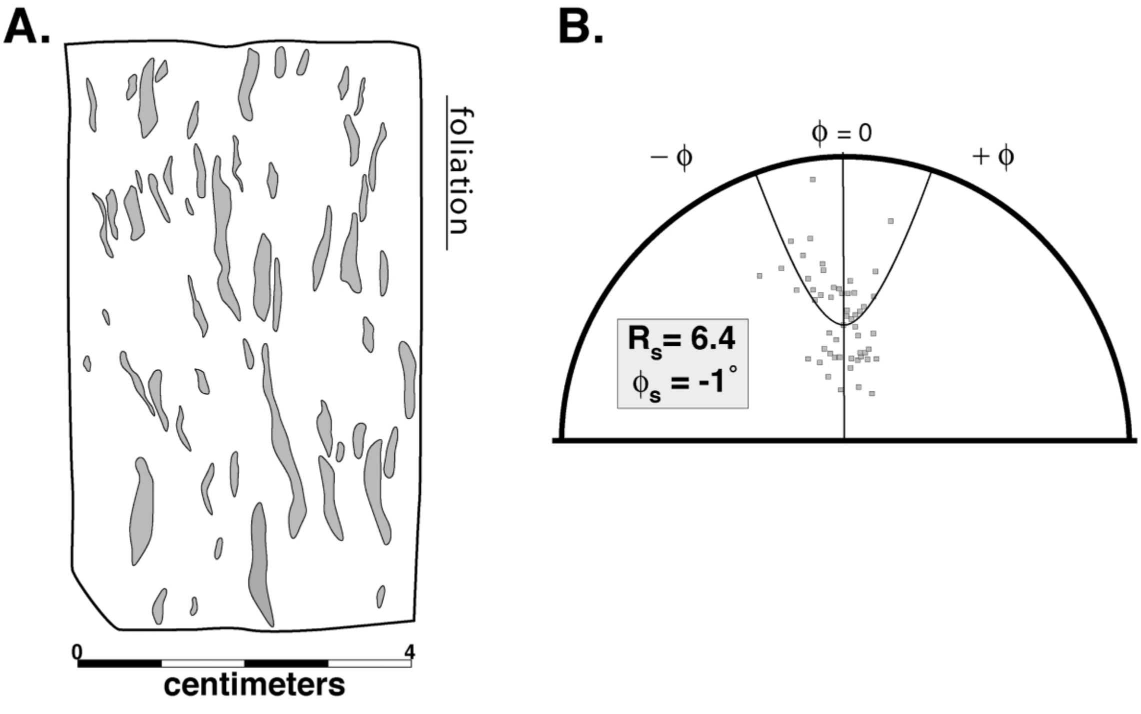

Fig. 4. (A) Tracing of quartz grain shapes in sample P22XZ. (B) R_f/ϕ_f hyperbolic stereogram of quartz grain shapes for sample P22XZ. $R_s = 6.4$ and $\phi_s = -1°$. ϕ_s is subparallel to the macroscopic foliation ($\phi = 0°$).

Table 1
Strain ratio (R_s), mean kinematic vorticity number (W_m), shear strain (γ), and three-dimensional strain data for Pinaleño Mountains high-strain zone. $R_s - XZ$ and $R_s - YZ$ measured from quartz grain shapes. X, Y, and Z calculated from $R_s - XZ$ and $R_s - YZ$ where $X = (R_s - XZ) \times (Z)$, $Y = 1$, $Z = 1/(R_s - YZ)$. $K = \mathrm{Ln}(X/Y)/\mathrm{Ln}(Y/Z)$

Sample	Rock type	Theta	$R_s - XZ$	W_m	γ	$R_s - YZ$	X	$Y0$	Z	XY	$R_s - YZ$	Ln(X/Y)	Ln(Y/Z)	K
P1	Protomylonite	10 ± 6	2.6	0.6 ± 0.2	1.0	1.6	1.63	1	0.63	1.63	1.60	0.49	0.47	1.03
P4	Protomylonite	9 ± 5	3.1	0.6 ± 0.2	1.0	2.0	1.55	1	0.50	1.55	2.00	0.44	0.69	0.63
P10	Protomylonite	14 ± 6	4.0	0.8 ± 0.15	1.9	1.4	2.86	1	0.71	2.86	1.40	1.05	0.34	3.12
P12	Mylonite	8 ± 5	5.0	0.6 ± 0.2	2.2	2.7	1.85	1	0.37	1.85	2.70	0.62	0.99	0.62
P20B	Mylonite gneiss	12 ± 4	4.4	0.8 ± 0.1	2.1	2.9	1.52	1	0.34	1.52	2.90	0.42	1.06	0.39
P22	Mylonite	17 ± 6	6.4	0.95 ± 0.05	2.7	2.1	3.05	1	0.48	3.05	2.10	1.11	0.74	1.50
P23	Mylonite	5 ± 4	8.3	0.6 ± 0.3	3.6	2.5	3.32	1	0.40	3.32	2.50	1.20	0.92	1.31
P30	Mylonite	7 ± 4	7.5	0.7 ± 0.2	3.4	2.6	2.88	1	0.38	2.88	2.60	1.06	0.96	1.11

protolith and mylonites consistent with isovolumetric deformation.

The relationship between the strain ratio (R_s) and the angle between the high-strain zone boundary and the long axis of the strain ellipsoid (θ) is a function of the mean kinematic vorticity of deformation (Fossen and Tikoff, 1993; Bailey et al., 1999). If R_s and θ are known, an estimate of W_m can be obtained. θ was estimated from the angular difference between (1) a sample's foliation and the high-strain zone boundary, and (2) the foliation and shear bands (C-surfaces), if present, in a sample. These values were averaged to obtain a mean θ. W_m values for eight samples ranged from 0.5 to 0.96 and plot off the R_s/θ curve for simple shear ($W_m = 1$) (Fig. 6). Error bars were estimated from the maximum and minimum θ values and the uncertainty associated with the dip (±3°) of the high-strain zone boundary (Fig. 6).

During general shear deformation, porphyroclasts rotate both forward and backward with respect to the overall flow (Simpson and De Paor, 1993). In ultramylonites, W_m can be estimated using the porphyroclast hyperbolic distribution (PHD) method (Simpson and De Paor, 1993). On a hyperbolic stereonet, forward and backward rotated grains define two separate fields separated by a hyperbola. Each limb of the hyperbola represents a flow apophysis and W_m is the cosine of the interlimb angle (Bobyarchick, 1986; Simpson and De Paor, 1993). Porphyroclasts in Pinaleño ultramylonites have rotated both forward and backward (Fig. 7). PHD analysis of three samples yield W_m values of 0.1–0.3 (Fig. 7, Table 2).

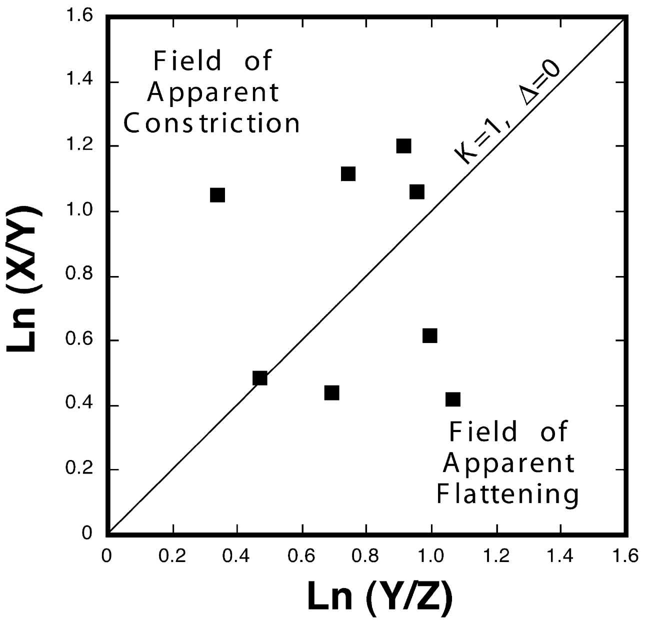

Fig. 5. Logarithmic Flinn diagram for quartz grain shapes.

4. Discussion

4.1. Deformation path of the Pinaleño Mountains high-strain zone

Vorticity analysis of mylonitic rocks from the Pinaleño Mountains metamorphic core complex indicates bulk general shear deformation ($W_m = 0.1–0.9$) that significantly deviated from simple shear. For protomylonites and

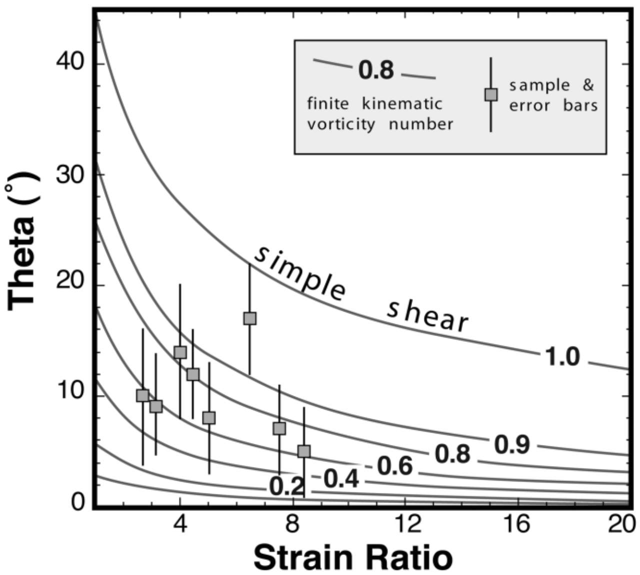

Fig. 6. R_s/Θ diagram for granitic protomylonites and mylonites. All samples plot within the field of general shear ($W_m = 0.4–0.96$).

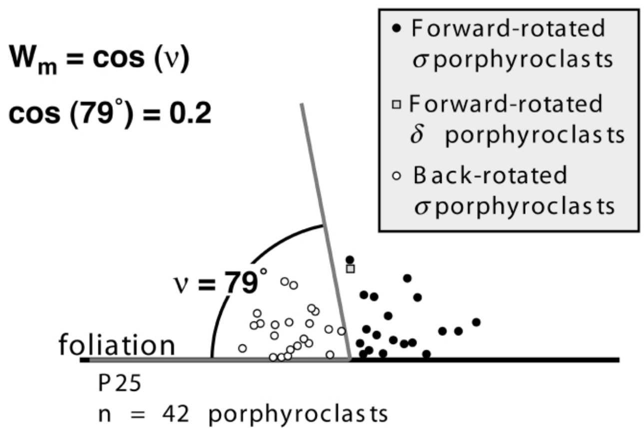

Fig. 7. Hyperbolic stereogram of feldspar porphyroclasts from ultramylonite (sample P25). Minimum hyperbola defines an opening angle of 79° and corresponds to $W_m = 0.2$.

mylonites to have experienced simple shear deformation, sectional strains ($R_s = 3-8$) of four to five times greater would be required (Fig. 6). The three-dimensional geometry (Fig. 8) of the Pinaleño mylonites approximates plane strain in the lengthening/thinning shear reference deformation of Tikoff and Fossen (1999). Symmetric structures were dominant on planes normal to the lineation and foliation, consistent with a bulk monoclinic symmetry for the deformation (Fig. 8). A minimum displacement of 2.2 km across the Pinaleño Mountains high-strain zone was calculated by integrating shear strains determined from sectional strains and the kinematic vorticity number of individual samples (Fig. 9). This estimate is lower than displacement estimates (3–7 km) of Naruk (1986, 1987) who assumed simple shear deformation. However, these estimates are clearly minimum values as the total displacement associated with narrow zones (< 10 cm) of ultramylonites and brittle faulting are not considered.

Ultramylonites record significantly lower W_m values (0.1–0.3) than protomylonites and mylonites (0.6–0.9) suggesting the Pinaleño Mountain high-strain zone experienced a non-steady vorticity history. There is, however, no obvious trend in W_m values for the protomylonites and mylonites, perhaps an indication that the bulk vorticity at low to moderate strains remained constant with time. Ultramylonites are composed of a weak matrix of mica and recrystallized quartz with isolated feldspar porphyroclasts, and may have experienced significant strain softening. A consequence of strain softening may be the development of

Table 2
Poryphyroclast hyperbolic distribution (PHD) data for Pinaleño Mountains high-strain zone ultramylonites. W_m = cosine (ν)

Sample	Total grains	Backrotated	ν-angle	W_m
P20B	30	17	71	0.3
P24	80	35	82	0.1
P25	42	22	79	0.2

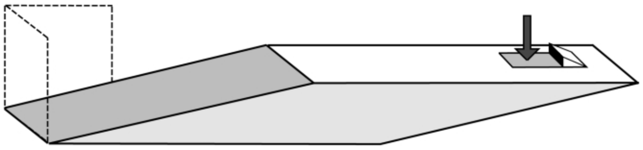

Fig. 8. Bulk plane strain, general shear deformation with a monoclinic symmetry for Pinaleño Mountains high-strain zone.

a large coaxial component of strain as the ultramylonite shortens more readily normal to foliation than protomylonitic to mylonitic rocks with a framework of interlocking feldspars.

Strain compatibility issues arise in zones of general shear deformation. Simpson and De Paor (1993) argued that general shear high-strain zones can develop only where: (1) the wall rock is capable of deforming, (2) sectional area changes (volume change) occur, along curved, non-parallel sided boundaries, or (3) the high-strain zone is separated from its wall rock by a fault or dilational gap. Hudleston (1999) noted that bulk strain compatibility might be achieved by arrays of anastomosing high-strain zones even if individually these zones locally deviate from plane strain and simple shear. Mylonitic rocks from the Pinaleño Mountains consistently record plane strain, general shear deformation and show few geochemical changes consistent with significant volume loss (Naruk, 1986). How then can this high-strain zone be compatible with its wall rocks? Possible solutions may include a non-parallel sided high-strain zone that widens at depth as well as a broad zone (at depth) of weakly deformed wall rocks in the footwall.

4.2. Evolution of fabrics in extensional core complexes

Lower plate materials in metamorphic core complexes are tectonically exhumed from mid-crustal depths during large-magnitude extension (e.g. Crittenden et al., 1980). Although a number of distinct models have been proposed to describe the geometry of highly extended terranes and metamorphic core complexes (Davis, 1983; Wernicke, 1985; Lister et al., 1986; Wernicke and Axen, 1988; Lister and Davis, 1989), all these models require that material in the lower plate is brought towards the surface during extension. Upper plate materials are commonly buried by alluvial deposits shed from the uplifted block.

At mid-crustal depths material in the lower plate experiences a state of stress in which the overburden component (σ_V) forms a larger component of the total stress than at upper levels in the crust (Fig. 10). As material is both deformed and translated towards the surface in a core complex high-strain zone, σ_V drops becoming a smaller component of the total stress (Fig. 10). Although the relationship between stress and the associated strain produced in rocks is complex, the decreasing σ_V should change the nature of the deformation path. In the mid-crust, large overburden stresses may cause deformation with a significant pure shear component; as σ_V drops the

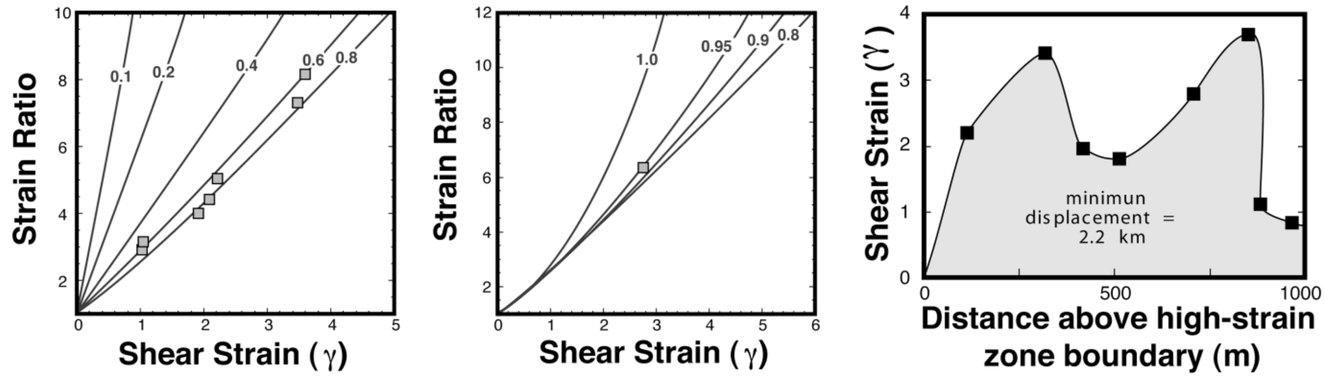

Fig. 9. Shear strains and minimum displacement estimate across the Pinaleño Mountains high-strain zone. R_s/γ curves from Bailey et al. (1999).

deformation becomes increasingly non-coaxial (Fig. 10). Rocks that begin to deform early in the history of a metamorphic core complex should record more of the coaxial deformation (lower W_m values) than rocks that start deforming later when the non-coaxial component is greater.

Early coaxial fabrics have been reported in a number of metamorphic core complexes (Compton, 1980; Miller et al., 1983; Lee et al., 1987; Wells and Allmendinger, 1990; Bestmann et al., 2000). Early coaxial fabrics in these core complexes are commonly overprinted by non-coaxial fabrics suggesting a non-steady vorticity path. Coaxial fabrics seem to be best preserved in ductily deformed supracrustal rocks (carbonates and quartzites) away from the main extensional high-strain zones. In contrast, granitic tectonites in metamorphic core complexes record non-coaxial fabrics (Davis, 1983; Reynolds, 1985; Naruk, 1986, 1987; this study). We view the coaxial and non-coaxial strains recorded in these metamorphic core complexes as evidence of a bulk general shear deformation path that evolves through time. If Pinaleño ultramylonites formed early in the deformation history their low W_m values relative to the protomylonites and mylonites may be consistent with an increasingly non-coaxial deformation path as the lower plate was denuded.

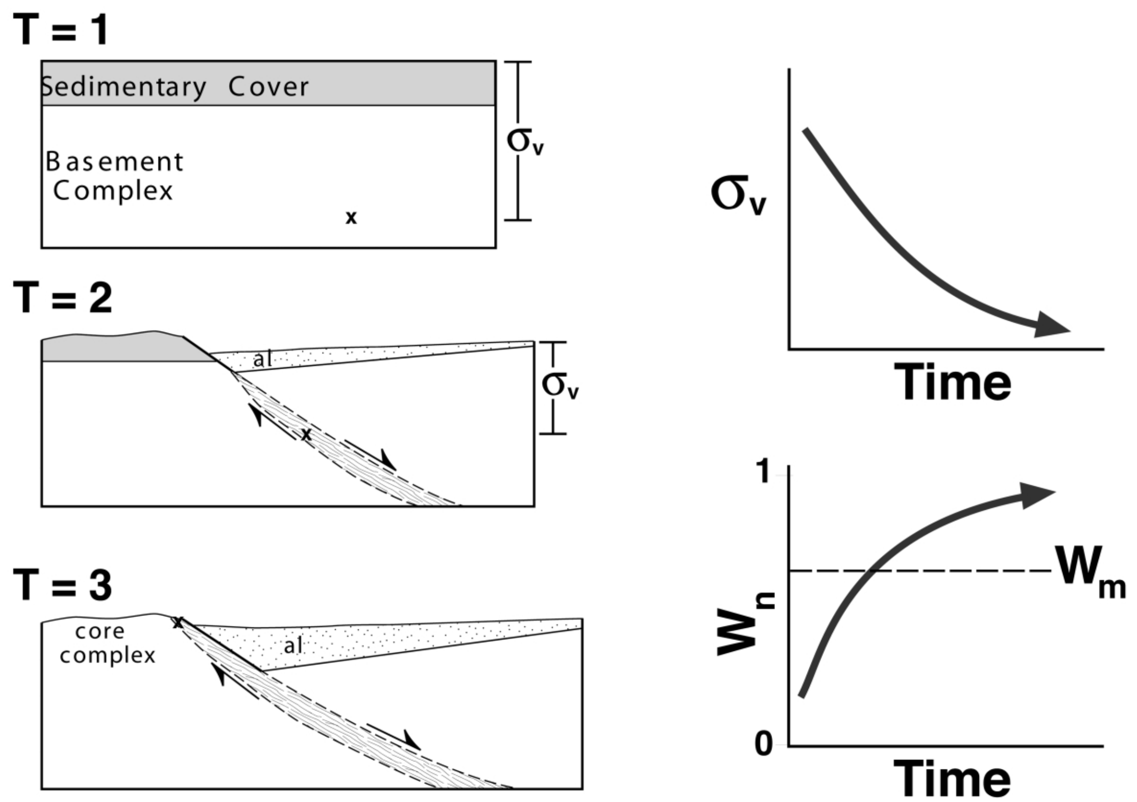

Fig. 10. Schematic diagram illustrating the progressive changes in the deformation path associated with the formation of extensional core complexes. Material at point X is deformed in core complex high-strain zone and is progressively uplifted to the surface. As σ_V decreases with time, the incremental vorticity (W_n) increases. Mean vorticity (W_m) records general shear.

5. Conclusions

Meaningful estimates of the mean vorticity and strain can be obtained from naturally deformed rocks. Although we cannot fully or uniquely understand the kinematic history of natural high-strain zones, quantitative strain and vorticity analyses place reasonable constraints on actual deformation paths. Granitic mylonites from the Pinaleño Mountains metamorphic core complex in southeastern Arizona experienced general shear deformation. W_m for protomylonites and mylonites ranged from 0.6 to 0.9, whereas ultramylonites record lower W_m values (0.1–0.3). The bulk deformation approximates plane strain with a monoclinic symmetry. We suggest that deformation in extensional core complexes records bulk general shear, not simple shear, and may progressively evolve from a significant pure shear component early in the deformation towards a larger simple shear component as the load on the footwall block is reduced during tectonic exhumation. This deformation path model for lower plate mylonites should be tested in other extensional metamorphic core complexes.

Acknowledgements

A William & Mary Faculty Research Grant to C.M. Bailey and a Chappell Summer Fellowship to E.L. Eyster provided financial support for this research. We thank S.E. Robinson for assistance in the field and B. Francis for insightful discussions. Helpful reviews were provided by Steve Ralser and Stephen Reynolds.

References

Bailey, C.M., Simpson, C., De Paor, D.G., 1994. Volume loss and tectonic flattening strain in granitic mylonites from the Blue Ridge province, Central Appalachians. Journal of Structural Geology 16, 1403–1416.

Bailey, C.M., Gilmer, A.K., Marquis, M.N., 1999. A tale of two shear zones: the vorticity and strain path of two greenschist facies shear zones. Geological Society of America Abstracts with Programs 31 (7), 59.

Beam, E.C., Fisher, D.M., 1999. An estimate of kinematic vorticity from rotated elongate porphyroblasts. Journal of Structural Geology 21, 1553–1559.

Bestmann, M., Kunze, K., Matthews, A., 2000. Evolution of a calcite marble shear zone on Thassos Island, Greece: microstructural and textural fabrics and their kinematic significance. Journal of Structural Geology 22, 1789–1807.

Bobyarchick, A., 1986. The eigenvalues of steady state flow in Mohr space. Tectonophysics 122, 35–51.

Compton, R.R., 1980. Fabrics and strains in quartzites of a metamorphic core complex, Raft River Mountains, Utah. In: Crittenden, M.D., Jr, Coney, P.J., Davis, G.H. (Eds.), Cordilleran Metamorphic Core Complexes. Geological Society of America Memoir 153, Boulder, CO, pp. 385–398.

Crittenden, M.D., Jr, Coney, P.J., Davis, G.H. (Eds.), 1980. Cordilleran Metamorphic Core Complexes. Geological Society of America Memoir 153, Boulder, CO.

Davis, G.A., Lister, G.S., Reynolds, S.J., 1986. Structural evolution of the Whipple and South mountains shear zones, southwestern United States. Geology 14, 7–10.

Davis, G.H., 1983. Shear-zone model for the origin of metamorphic core complexes. Geology 11, 342–347.

Davis, G.H., Naruk, S.J., Thorman, C.H., 1988. Structural geology of the Rincon and Pinaleño metamorphic core complexes, southeast Arizona. State of Arizona Bureau of Geology and Mineral Technology Special Paper 5, 249–259.

De Paor, D.G., 1988. R_f/ϕ strain analysis using an orientation net. Journal of Structural Geology 10, 323–333.

Fletcher, J.M., Bartley, J.M., 1994. Constrictional strain in a non-coaxial shear zone: implications for fold and rock fabric development, central Mojave metamorphic core complex, California. Journal of Structural Geology 16, 555–570.

Fossen, H., Tikoff, B., 1993. The deformation matrix for simultaneous simple shearing, pure shearing and volume change, and its application to transpression–transtension tectonics. Journal of Structural Geology 15, 413–422.

Hirth, G., Tullis, J., 1992. Dislocation creep regimes in quartz aggregates. Journal of Structural Geology 14, 145–159.

Hudleston, P., 1999. Strain compability and shear zones: is there a problem? Journal of Structural Geology 21, 923–932.

Jiang, D., Williams, P.F., 1998. High-strain zones: a unified model. Journal of Structural Geology 20, 1105–1120.

Kruger, J.M., Johnson, R.A., 1994. Raft model of crustal extension: evidence from seismic reflection data in southeast Arizona. Geology 22, 351–354.

Lee, J., Miller, E.L., Sutter, J.F., 1987. Ductile strain and metamorphism in an extensional tectonic setting: a case study from the northern Snake Range, Nevada, USA. In: Coward, M.P., Dewey, J.F., Hancock, P.L. (Eds.), Continental Extensional Tectonics. Geological Society Special Publications 28, pp. 267–298.

Lin, S., Jiang, D., Williams, P.F., 1998. Transpression (or transtension) zones of triclinic symmetry: natural example and theoretical modelling. In: Holdsworth, R.E., Strachan, R.A., Dewey, J.F. (Eds.), Continental Transpressional and Transtensional Tectonics. Geological Society Special Publications 135, pp. 41–57.

Lister, G.S., Davis, G.A., 1989. The origin of metamorphic core complexes and detachment faults formed during Tertiary continental extension in the northern Colorado River region, USA. Journal of Structural Geology 11, 65–94.

Lister, G.S., Etheridge, M.A., Symonds, P.A., 1986. Application of the detachment fault model to the formation of passive continental margins. Geology 14, 286–290.

Long, K.B., Baldwin, S.L., Gehrels, G.E., 1995. Tectonothermal evolution of the Pinaleño–Jackson Mountain core complex, southeast Arizona. Geological Society of America Bulletin 107, 1231–1240.

Mawer, C.K., 1983. State of strain in a quartzite mylonite, Central Australia. Journal of Structural Geology 5, 401–409.

Miller, E.L., Gans, P.B., Garing, J., 1983. The Snake range décollement: an exhumed mid-Tertiary brittle-ductile transition. Tectonics 2, 239–263.

Naruk, S.J., 1983. Calculation of shear strain and translation values from mylonitic gneiss in a metamorphic core complex. M.S. thesis, University of Arizona.

Naruk, S.J., 1986. Strain and displacement across the Pinaleño Mountains shear zone, Arizona, USA. Journal of Structural Geology 8, 35–46.

Naruk, S.J., 1987. Displacement calculations across a metamorphic core complex mylonite zone: Pinaleño Mountains, southeastern Arizona. Geology 15, 656–660.

O'Hara, K., 1990. State of strain in mylonites from the western Blue Ridge province, southern Appalachians: the role of volume loss. Journal of Structural Geology 12, 419–430.

Passchier, C.W., 1987. Stable positions of rigid objects in non-coaxial flow: a study in vorticity analysis. Journal of Structural Geology 9, 679–690.

Passchier, C.W., 1988a. Analysis of deformation paths in shear zones. Geologische Rundschau 77, 309–318.

Passchier, C.W., 1988b. The use of Mohr circles to describe non-coaxial progressive deformation. Tectonophysics 149, 323–338.

Passchier, C.W., Urai, J.L., 1988. Vorticity and strain analysis using Mohr diagrams. Journal of Structural Geology 10, 755–763.

Reynolds, S.J., 1985. Geology of the South Mountains, central Arizona. Arizona Bureau of Geology and Mineral Technology Bulletin 195, 61.

Simpson, C., Wintsch, R.P., 1989. Evidence for deformation induced K-feldspar replacement by myrmekite. Journal of Metamorphic Geology 7, 261–275.

Simpson, C., De Paor, D.G., 1993. Strain and kinematic analysis in general shear zones. Journal of Structural Geology 15, 1–20.

Simpson, C., De Paor, D.G., 1997. Practical analysis of general shear zones using the porphyroclast hyperbolic distribution method: an example from the Scandinavian Caledonides. In: Sengupta, S., (Ed.), Evolution of Geological Structures in Micro- to Macro- Scales, Chapman & Hall, pp. 169–184.

Thorman, C.H., 1982. Geology of the Pinaleño Mountains, Arizona: a preliminary report. Arizona Geological Society Digest 13, 5–12.

Tikoff, B., Fossen, H., 1995. The limitations of three-dimensional kinematic vorticity analysis. Journal of Structural Geology 17, 1771–1784.

Tikoff, B., Fossen, H., 1999. Three-dimensional reference deformations and strain facies. Journal of Structural Geology 21, 1497–1512.

Tikoff, B., Teyssier, C., 1994. Strain and fabric analyses based on porphyroclast interaction. Journal of Structural Geology 16, 477–491.

Tullis, J., 1983. Deformation of feldspars. In: Ribbe P.H. (Ed.), Feldspar Mineralogy. Mineralogical Society of America Reviews in Mineralogy 2, pp. 297–323.

Tullis, J., Yund, R.A., 1985. Dynamic recrystallization of feldspar: a mechanism for ductile shear zone formation. Geology 13, 238–241.

Tullis, J., Yund, R.A., 1987. Transition from cataclastic flow to dislocation creep of feldspar: mechanisms and microstructures. Geology 15, 606–609.

Wallis, S.R., 1992. Vorticity analysis in a metachert from the Sanbagawa belt, SW Japan. Journal of Structural Geology 14, 271–280.

Wells, M.L., Allmendinger, R.W., 1990. An early history of pure shear in the upper plate of the raft River metamorphic core complex: Black Pine Mountains, southern Idaho. Journal of Structural Geology 12, 851–867.

Wenk, H.-R., Pannetier, J., 1990. Texture development in deformed granodiorites from the Santa Rosa mylonite zone, southern California. Journal of Structural Geology 12, 177–184.

Wernicke, B.P., 1985. Uniform-sense simple shear of the continental lithosphere. Canadian Journal of Earth Sciences 22, 108–125.

Wernicke, B.P., Axen, G.J., 1988. On the role of isostasy in the evolution of normal fault systems. Geology 16, 848–851.